Journal of Engineering and Applied Sciences
MEDWELL PUBLICATIONS

Optimization of Nonlinear Differential Equations for Defining One Leg Human Locomotion

Abdalftah Elbori and Ali Albasher Gumma Albarki
Department of Mathematics, Faculty of Science, Azzaytuna University, Tarhuna, Libya

Key words: Central Patterns Generators (CPGs), modeling of one leg of human, stability analysis, optimizing nonlinear differential equations, real data

Corresponding Author:
Abdalftah Elbori
Department of Mathematics, Faculty of Science, Azzaytuna University, Tarhuna, Libya

Page No.: 3674-3683
Volume: 15, Issue 22, 2020
ISSN: 1816-949x
Journal of Engineering and Applied Sciences

Abstract: This study discusses how to optimize the Bidirectional of the Central Pattern Generators (CPGs) to produce rhythmic patterns for human locomotion by using the enhancement Genetic algorithm and pattern search function. It also shows how small changes in some CPG parameters in stable domain result in different walking gaits, optimizing bidirectional two CPGs in stable domain do not only enhance movement but also generate rhythmic patterns similar to the rhythmic patterns derived from real data without any input or sensory feedback.

INTRODUCTION

To begin with, CPGs are neural networks located in the spinal cord of vertebrate as well as invertebrate animals. These CPGs are designed to exclusively supply synchronized rhythmic pattern activities, viz., leg movement in the course of walking, respiration or chewing[1]. One of the captivating characteristics of CPGs lies in their capacity to generate rhythmic signals over and above any rhythmic contribution from higher control centers or sensory response. In addition, CPGs are vigorous, versatile and effortlessly adjustable. These compelling attributes render CPGs expedient for mobility control of robots with multiple joints, Degrees of Freedom (DOF) and even for kinematically redundant robots. Research into bio-robotics has recently gained unprecedented momentum. The interest in the application of robots to enhance traditional mechatronics systems or to attend to particular issues related to biology has brought bio-robotics back to life but with a different spirit[1]. The focus now is on how in robotics, CPGs can be effectively manipulated to administer cadenced movements related to crawling, flying and swimming and not only legged walking (for more details)[1, 2]. A plethora of studies on CPGs have introduced fascinating results. Some of these studies have indicated that CPGs can in fact control some functions in the human body, viz., breathing and digestion[2, 3]. Other studies, based on the suppressive or stimulatory connection between the extensor neuron and the flexor neuron[4, 5] have revealed the potential of modelling a variety of physical structures of the limbs and arms of robots[6-10] by copying the control systems of robots. This endeavor is based on the premise that CPGs will simultaneously start to orchestrate and send gestures to neurons once the body begins to move[11, 12]. The ultimate goal of such studies is to produce rhythmic patterns in robots akin to those existing in reality. A rather inspiring endeavor in recent years has focused on how CPGs can account for different modes of locomotion. Research into insect kinesis has given rise to a variety of CPG setups utilized in octopod and hexapod robots[11, 12]. Other CPGs setups have been manipulated to

manage swimming robots, viz., eel robots or swimming lampreys[13, 14]. Finally, some CPG configurations have been utilized to control biped locomotion in humanoid robots[15-21].

In view of the studies mentioned above, this study explores the effect of optimizing bidirectional two CPGs on the performance of one-leg movement of humans by using Genetic Algorithm (GA) and pattern search. First, the paper examines the kinematics of human locomotion utilized in simulations and gait setups by depending on Tema Motion software. Second, it mentions to Uncouple, Unidirectional and bidirectional two CPGs. Third, it probes the stability of the three cases CPGs under investigation. Fourthly, optimizing bidirectional two CPG structures to generate rhythmic patterns for one human's leg with two and three degrees of freedom. The paper concludes that an optimizing of bidirectional two CPGs may equally produce similar results to the rhythmic patterns that obtain from real data. Fifthly, this study focuses on the effective parameters in CPGs. Finally, the paper draws conclusions and offers suggestions for future research.

MATERIALS AND METHODS

Kinematic analysis and modeling of biped locomotion systems: Presumably, collecting the real data is the shortest and most straightforward method to produce a CPG-induced acceleration motion trajectory for biped locomotion. In order to determine the kinematic attributes with the system behavior while walking, we first use the rubrics of biped kinematics on the sagittal plane to outline the simple kinematic precepts of robotic bipedal locomotion with two or three DOFs[22, 23]. A comparison of the acceleration or forward motion trajectory gleaned from the real data with CPGs will be simultaneously drawn. Figure 1 illustrates how CPGs are used to produce rhythmic patterns for the hip, knee and ankle angles via one leg of a human when the lower body is parallel to the ground. It is worth mentioning here that the results obtained are contingent upon the manner in which CPGs are analyzed.

A closer look into the kinematics of the hip, knee and ankle angles in the swing phase reveals the following basic kinematics equations: From the joint between hip and knee and from the joint between knee and ankle, we have. The first coordinate (x_1, y_1) yields $x_1 = x_d+L_1\cos\theta_1$ and $y_1 = y_d+L_1\sin\theta_1$. The second coordinate (x_2, y_2) reveals that $x_2 = x_d+L_1\cos\theta_1+L_2\cos\theta_2$ and $y_2 = y_d+L_1\sin\theta_1+L_2\sin\theta_2$ and the third coordinate (x_3, y_3) translates into:

$$x_3 = x_2+L_3\cos\theta_3 \text{ and } y_3 = y_2+L_3\sin\theta_3$$

where, x_d is the proceeding displacement (i.e., the distance during locomotion) and y_d stands for the positive direction

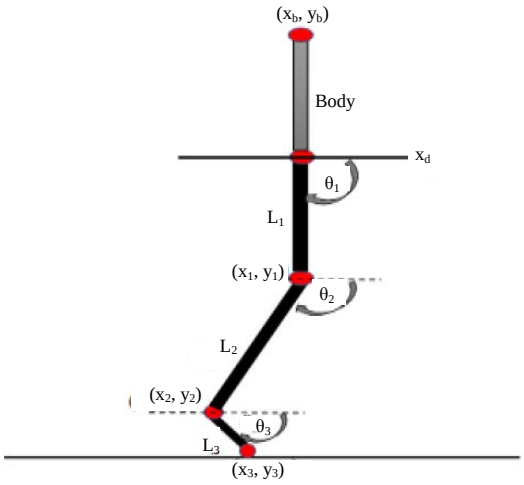

Fig. 1: The Planar biped model when the lower body is parallel to the ground

of the hip height at each step. L_1, L_2 and L_3 represent three lengths: from the hip joint to the knee joint, from the knee joint to the ankle joint and from the ankle joint to the end effector, respectively. The angles, θ_1, θ_2 and θ_3 which represent the hip, knee and ankle angles, respectively, will acquire their rhythmic patterns from CPGs. With regard to y_d, it is assumed to be zero when the lower body is parallel to the ground. The researchers in this study, however, fixed the hip joint in spite of the fact that the hip joint was not fixed when collecting real data.

Central Pattern Generators (CPGs): We have already defined CPGs as inspired networks of nonlinear bipolar neurons capable of generating rhythmic patterns without providing input from higher control centers. Indeed, many an application has been conducted using numerous different neutrals in robotics. Such neutrals have been put into action via software methods, called CPGs. The CPG unit is accountable for producing the angular locus that is vital for the hip and knee joints. These CPGs are supported in mathematical equations and presented in general formulas. This process is generally referred to as the standalone nonlinear oscillator. In keeping with a number of experiments, Marbuch and Van den Kieboom claim that sinusoidal signals appear to be compatible with locomotion control[9, 21, 24]. For instance, let us consider the following equation:

$$x = A\sin(2\pi ft+\varphi)$$

Where:
A = The amplitude
f and φ = The frequency and phase, respectively

Now, by taking the first and second derivatives of x, a first order differential equation can be derived:

$$\tau\dot{x} = v,\ \tau\dot{v} = -x$$

where, $\tau = 1/2\pi f$. A closer examination of this linear differential equation gives us an inferential characterization of the amplitude A. It is important to note here that A is subject to the fundamental settings conditions, suggesting that it may be affected to a certain extent by variations in the state variables. It is highly recommended, therefore, to add a new term that would propel the system to a limit cycle with an accurate amplitude. To that end, the addition of this new term will produce the following differential equation:

$$\left.\begin{aligned}\tau\dot{x} &= v\\ \tau\dot{v} &= -x-\frac{\alpha}{E}(x^2+v^2-E)v-x\end{aligned}\right\} \quad (1)$$

In Eq. 1 above, the parameters τ, α and E are positive criteria. The bearing x^2+v^2 serves as the definitive energy of the oscillator and the aspect x^2+v^2-E is the energy error of the oscillator. Because of this, the nonlinear term may be presumed as the normalized energy error multiplied by α and v. The positive parameter a may be utilized to coordinate the attracting force to the limit cycle. In this case, the larger α, the faster the convergence will be. Equation 2 delineates the system for these types of oscillators:

$$\left.\begin{aligned}\tau\dot{x}_i &= v_i\\ \tau\dot{v}_i &= -\frac{\alpha}{E_i}(x_i^2+v_i^2-E_i)v_i-x_i+\sum_j\left(\frac{a_{ij}x_j+b_{ij}v_j}{\sqrt{x_j^2+v_j^2}}\right)\end{aligned}\right\} \quad (2)$$

where, a_{ij} and b_{ij} are positive constants that designate the manner of the impact of oscillator j on the oscillator i, importing a specific phase difference into the limit cycle. However, certain structures of outputs may appear by virtue of changing the numerical values of the parameters[21, 25]. Interestingly, drawing on the system of differential Eq. 2 above unfolds three kinds of CPGs, namely Uncoupled, unidirectional and bidirectional two CPGs. By assuming $x_1 = \theta_1$, $x_2 = \theta_2$ and $x_3 = \theta_3$ where θ_1, θ_2 and θ_3 stand for the angular positions of the hip, knee and the ankle, respectively.

RESULTS AND DISCUSSION

Stability analysis

Uncoupled two CPGs: Economically speaking, uncoupled two CPGs comprise four differential equations. Equation 3 below delineates the system of these equations:

$$\left.\begin{aligned}\tau\dot{x}_1 &= v_1\\ \tau\dot{v}_1 &= -\frac{\alpha}{E_1}(x_1^2+v_1^2-E_1)v_1-x_1\\ \tau\dot{x}_2 &= v_2\\ \tau\dot{v}_2 &= -\frac{\alpha}{E_2}(x_2^2+v_2^2-E_2)v_2-x_2\end{aligned}\right\} \quad (3)$$

The four differential equations above correspond to two CPGs. Given that the first CPG and the second CPG are independent of each other, the stability of this system discussed in more details[21].

Unidirectional two CPGs: In a similar manner, unidirectional two CPGs comprise four differential equations laid out by the system of the differential Eq. 4:

$$\left.\begin{aligned}\tau\dot{x}_1 &= v_1\\ \tau\dot{v}_1 &= -\frac{\alpha}{E_1}(x_1^2+v_1^2-E_1)v_1-x_1+\frac{a_{12}x_2+b_{12}v_2}{\sqrt{x_2^2+v_2^2}}\\ \tau\dot{x}_2 &= v_2\\ \tau\dot{v}_2 &= -\frac{\alpha}{E_2}(x_2^2+v_2^2-E_2)v_2-x_2\end{aligned}\right\} \quad (4)$$

These four differential equations represent two CPGs. The first CPG is designated by the first and second equations and the second CPG the third and fourth equations for stability in more details[21].

Bidirectional two CPGs: Bidirectional two CPGs constitute the system of four differential equations as displayed in Eq. 5 which embody two CPGs. The first CPG reflects the first and second equations and the second CPG describes the third and fourth equations:

$$\left.\begin{aligned}\tau\dot{x}_1 &= v_1\\ \tau\dot{v}_1 &= -\frac{\alpha}{E_1}(x_1^2+v_1^2-E_1)v_1-x_1+\frac{a_{12}x_2+b_{12}v_2}{\sqrt{x_2^2+v_2^2}}\\ \tau\dot{x}_2 &= v_2\\ \tau\dot{v}_2 &= -\frac{\alpha}{E_2}(x_2^2+v_2^2-E_2)v_2-x_2+\frac{a_{21}x_2+b_{21}v_1}{\sqrt{x_1^2+v_1^2}}\end{aligned}\right\} \quad (5)$$

Stability for bidirectional two CPGs is discussed in more details[21]. According to this study indicates that the bidireccional coupling yields the best performance level. Results also reveal that when $\mu = \mu_1 = \mu_2 = \alpha/E_1 = \alpha/E_2$ and $\tau = \tau_1 = \tau_2$ are close to zero and the fixed points are stable, the velocity and displacement increase. That is, changes in the CPG parameters may produce different results. Of course, it is not only the value of both parameters τ and α are important but also in the bidirectional two CPGs, the couple weight a_{ij} and b_{ij} that drive the system to two diverging phases which lead to

Fig. 2: Video-recorded data and high-speed camera

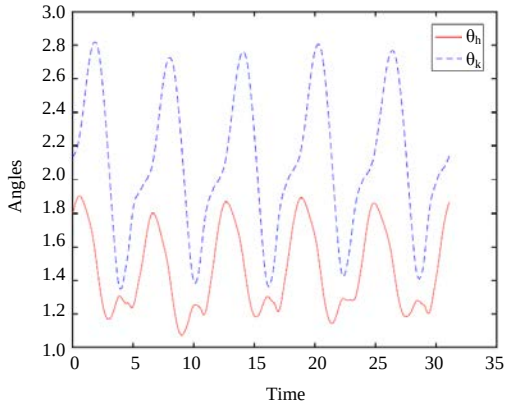

Fig. 3: Angles of the hip and knee that are collected by real data

obtain the conflicting perturbations, these perturbations are influenced by the energies E_j of bidirectional two CPGs. The rhythmic motions rely on coupling weights a_{ij} and b_{ij} and the values of both parameters τ and α[21].

Obtaining real data: Obtaining real data involves different objectives. One of the major objectives, for instance, is to learn whether the output of CPGs may be endorsed. Another important and legitimate inquiry is whether manipulating CPGs would establish rhythmic patterns for the hip, knee and ankle angles akin to those seen in nature. Figure 2 explain how real data can be obtained under different circumstances along with their analysis. The data were obtained through video recording by using high speed camera as described in Fig. 2.

In fact, in order for us to be able to analyze the video-recorded real data, the researchers used the Tema Motion software. Results of using Tema Motion to establish real data for the hip and knee angles are shown in Fig. 3 and for the hip, knee and ankle angles are shown in Fig. 4 where θ_h, θ_k and θ_a stand for the angles of hip, knee and ankle of the real data, respectively.

Optimizing CPGs: Our aim here is to Compare the real data with optimizing bidirectional two CPGs in order to generate rhythmic motions similar to those, we see in

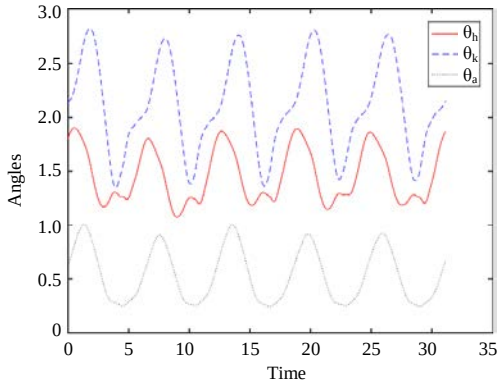

Fig. 4: Angles of the hip, knee and ankle that are collected by real data

natural human locomotion. Presumably, part of evaluating gait patterns is optimizing the CPGs in order to obtain optimal parameter sets. Put differently, it is vital that we recognize how the angular positions of the hip and knee may change in time in order to produce motion along the x-direction. Recall that each pattern generator produces angular patterns for each joint. There are three cases to consider here. The parameter sets for the CPG of each joint are given below for the bidirectional two CPGs is $P = \{\tau, \alpha, E_1, E_2, a_{12}, b_{12}, a_{21}, b_{21}\}$, other cases uncoupled and unidirectional CPGs are Cancelled here according to studying[21]. In order to determine the optimal parameter sets by manipulating the Genetic algorithm, this study endeavors to utilize more than one cost function. The first cost function can be written as:

$$J_1 = \sum_{k=1}^{m}((\theta_1(k)-\theta_h(k))^2+(\theta_2(k)-\theta_k(k)^2) \quad (6)$$

Translating the aforementioned equation into words indicates that θ_1 and θ_2 are the outputs of the CPGs as defined before where θ_h and θ_k are the angles of hip and knee of the real data respectively and that n is the total number of step times. The conclusive goal here is to minimize differences between the outputs of the CPGs and the real data for the angles of the hip and the knee in the region captured by stability analysis[21]. In addition, the equation above unfolds two constraints, namely $0 \leq 1\theta_1$, $\theta_2 \leq \pi$. In the present study, a hybrid function was used during the optimization process, an optimization function that runs after the GA terminates in order to improve the value of the fitness function. The significance of the hybrid function stems from the fact that it uses the final point from the GA as its initial point which can be specified in the hybrid function options.

In particular, the present study draws on the optimization Toolbox function for pattern searches or fmincon a constrained minimization function. Of course,

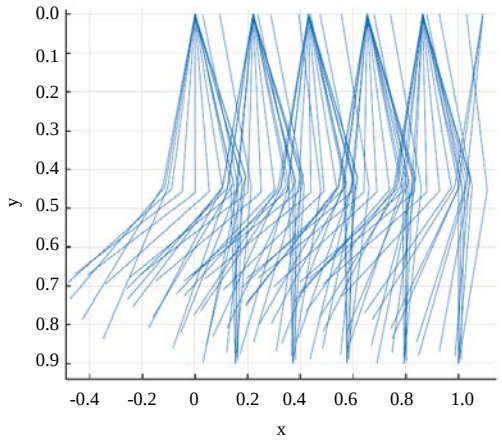

Fig. 5: One leg animation for the CPGs corresponding to the values α = 0.0010, τ = 0.9624, E_1 = 0.4721, a_{12} = 1.6071, b_{12} = 0.0288, E_2 = 1.3746, a_{21} = 2.1200, b_{21} = -0.0479 and the initial conditions, $x_1(0)$ = 1.8139, $v_1(0)$ = 0.1369, $x_2(0)$ = 2.1081, $v_1(0)$ = 0.5569

manipulating this Toolbox function necessitates initially running the GA to target a point close to the optimal point and hence to use that point as the initial mark for a pattern search or fmincon. With respect to the stability part, it is predicated on the fact that the leg would not be able to move when cases of the uncoupled and unidirectional two CPGs are applied to simple kinematic equations. In contrast, locomotion is predicted to occur when bidirectional two CPGs are applied with constraints to the joint angles between [0, π]. The conclusive objective of optimizing the CPGs and applying the objective function in Eq. 6 was to minimize the error between the real data and the outputs of the CPGs. To decrease the error, we set the initial conditions in the CPGs as variables which are determined by GA optimization and where the mutation rate and crossover fraction are predicted to be 0.05 and 0.2, respectively. As described in Fig. 5-8. (x_{2c}, y_{2c}) and (x_{2r}, y_{2r}) are the second coordinates of one leg using output of CPGs and real data, respectively.

e_1 and e_2 are the errors between each angle, respectively. Remarkably, concentrating on three joints with three DOFs of the ankle, knee and hip angles and using the same technique above, we succeeded in obtaining the real data for the three angles as shown in Fig. 4. Adding the ankle angle obtained from real data in the objective function yielded the following new objective function:

$$J_2 = J_1 \sum_{k=1}^{n} ((\theta_3(k)-\theta_a(k))^2) \quad (7)$$

Where:

θ_3 = The output of the third CPG for the angle of the ankle

θ_a = The angle of the ankle obtained from the real data

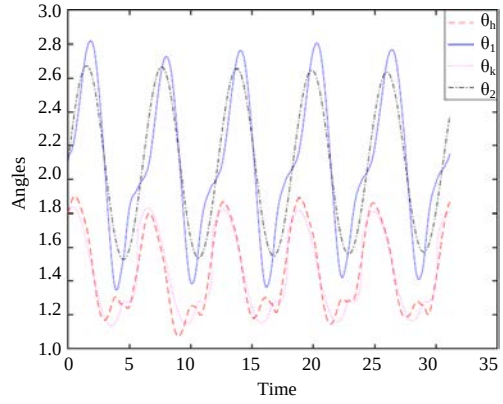

Fig. 6: Outputs of the CPGs and real data: The outputs of the CPGs correspond to the same values in Fig. 5

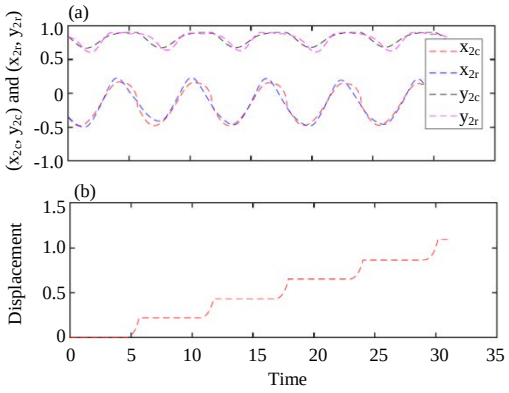

Fig. 7(a, b): Coordinates of the knee joint and displacement against time

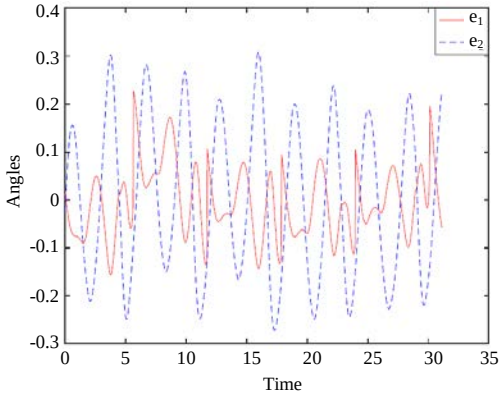

Fig. 8: Errors between the outputs of the CPGs and the real data at each angle corresponding to the same values in Fig. 5

For the last CPG different couplings may be used. In this study, for the ankle joint we use two CPGs coupled bidirectionally and we take only one output, followed by optimizing the objective function J_2. The results are

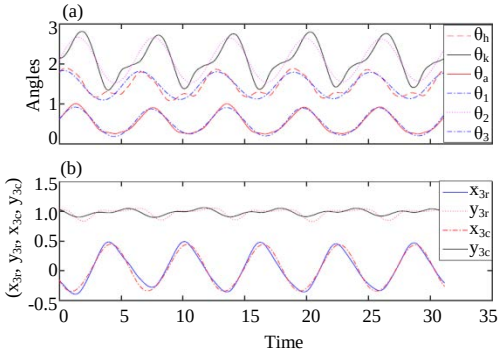

Fig. 9(a, b): Angles of both the CPGs and real data with horizontal axis

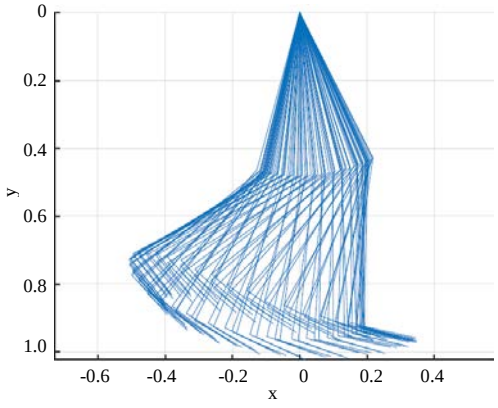

Fig. 10: One leg animation with three DOFs in swing phase corresponding to the same values in Fig. 9

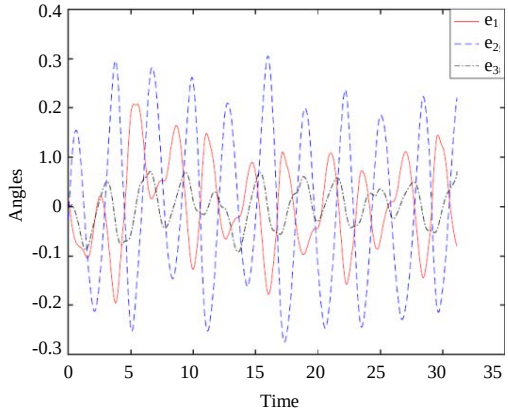

Fig. 11: Errors between the outputs of the CPGs and the real data at each angle corresponding to the same values in Fig. 9

shown in Fig. 9-11. Note that, the outputs of the CPGs are close to those coming from the real data, although, the hip joint being fixed. The outputs correspond to the values $\alpha = 0.0024$, $\tau = 0.9601$, $E_1 = 0.1989$, $a_{12} = 1.4845$,

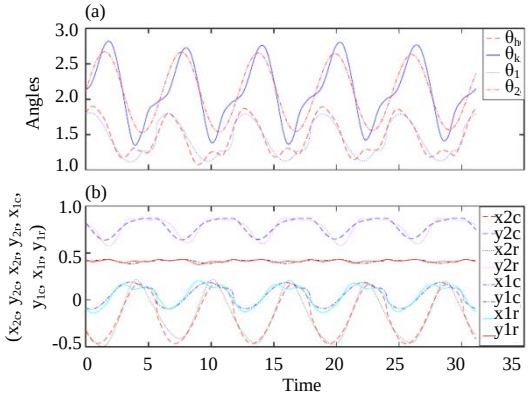

Fig. 12(a, b): Angles of the hip and knee using the outputs of the CPGs and the real data: the outputs of CPGs correspond to the values $\alpha = 0.0012$, $\tau = 0.9617$, $E_1 = 0.2003$, $a_{12} = 1.4789$, $b_{12} = 0.0478$, $E_2 = 5.9966$, $a_{21} = 2.1212$, $b_{21} = -0.0512$ and the initial condition $x_1(0) = 1.7785$, $v_1(0) = 0.1390$, $x_2(0) = 2.1075$, $v_2(0) = 0.5540$

$b_{12} = 0.0614$, $E_2 = 5.000$, $a_{21} = 2.1210$, $b_{21} = -0.0586$ and the initial condition $x_1(0) = 1.8135$, $v_1(0) = 0.1390$, $x_2(0) = 2.1075$, $v_2(0) = 0.5540$, for the first two CPGs and $\alpha_1 = 0.3653$, $\tau_1 = 0.9623$, $E_3 = 1.2259$, $a_{34} = 0.6486$, $b_{34} = 0.0331$, $E_4 = 3.0105$, $a_{43} = 1.6668$, $b_{43} = -0.0054$ and the initial condition $x_3(0) = 0.6162$, $v_3(0) = 0.3347$, $x_4(0) = 0.4661$, $v_4(0) = 0.0174$ for the last two CPGs. Where e_1, e_2 and e_3 are the errors between each angle, respectively in Fig. 11.

In order to reduce the error between the real data and the outputs of the bidirectional two CPGs in one leg with 2 DOFs, we should optimize the objective function below:

$$J_3 = J_1 + \sum_{k=1}^{n}((x_{2c}(k)-x_{2r}(k))^2)+ (y_{2c}(k)-y_{2r}(k))^2) \quad (8)$$

where, (x_{1c}, y_{1c}), (x_{2c}, y_{2c}), (x_{1r}, y_{1r}) and (x_{2r}, y_{2r}) are the coordinates that are generated from the outputs of the CPGs and real data during locomotion. The CPGs are able to generate the RPs similar to the outputs of the real data. The results of the optimization are shown in Fig. 12-15. The objective function J_3 indicates that the standard deviation or the error between the outputs of the bidirectional two CPGs and real data are decreased compared with the previous case for one leg with two DOFs. Despite the fact that the error still exists in this case, the outputs of the CPGs corresponds to the same values of the parameters which applies our conditions of the stability of the bidirectional two CPGs.

However, to optimize the model with three joints, it is highly recommended that we use the objective function in Eq. 9:

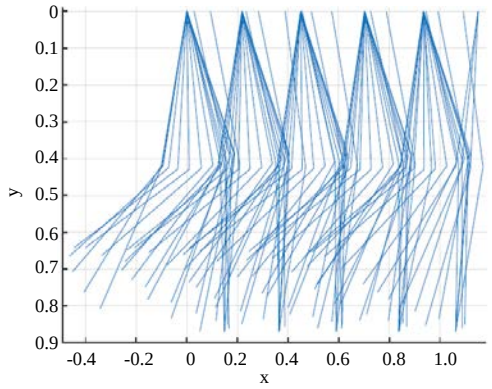

Fig. 13: Animation of one leg with 2 DOFs corresponding to the same values in Fig. 12

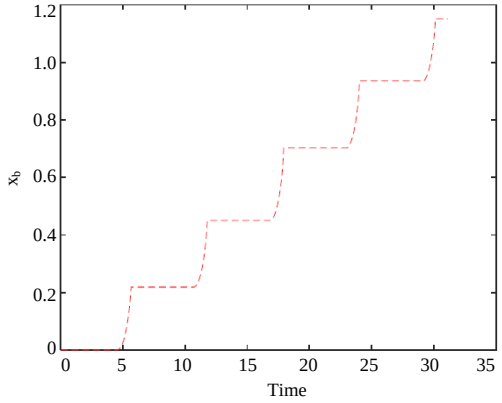

Fig. 14: Displacement against time corresponding to the same values in Fig. 12

$$J_4 = J_3 + \sum_{k=1}^{n} ((\theta_3(k)-\theta_{Ar}(k))^2 + (x_{3c}(k)-x_{3r}(k))^2 + (y_{3c}(k)-y_{3r}(k))^2) \quad (9)$$

where, (x_{3c}, y_{3c}) and (x_{3r}, y_{3r}) are horizontal axes that are generated outputs from CPGs and real data during locomotion. The results of the optimization are shown by Fig. 16 and 17.

Unlike the other cases-induced results, these results have improved greatly when using the bidirectional two CPGs. Remarkably, this type of CPGs, the bidirectional two CPGs has generated rhythmic patterns that are closest to those derived from the real data by using GA and pattern search solvers. Most importantly, this type of CPGs has revealed the best results compared to all other types of CPGs thus far available up to day.

Effective parameters in CPGs: In this part of the study, we attempted to optimize the parameters of the CPGs with the objective of determining the operational parameters in the bidirectional two CPGs. The results reveal that the

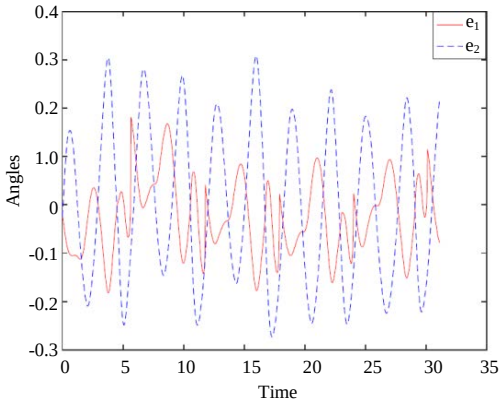

Fig. 15: Errors between the outputs of the CPGs and the real data at each angle corresponding to the same values in Fig. 12

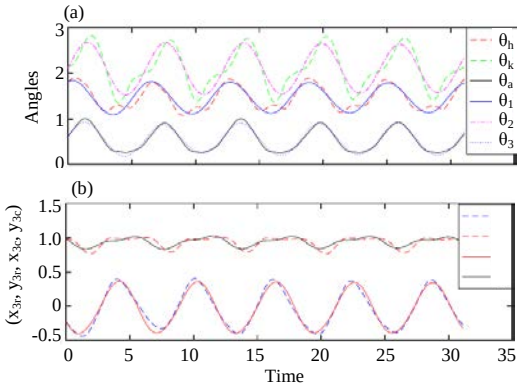

Fig. 16(a, b): Angles of the hip, knee and ankle using the outputs of the CPGs and the real data: the outputs of the CPGs correspond to values $\alpha = 0.0023$, $\tau = 0.9599$, $E_1 = 0.2020$, $a_{12} = 1.4808$, $b_{12} = 0.0582$, $E_2 = 4.9724$, $a_{21} = 2.1238$, $b_{21} = -0.0612$ and the initial condition $x_1(0) = 1.8135$, $v_1(0) = 0.1390$, $x_2(0) = 2.1075$, $v_2(0) = 0.5540$, for the first two CPGs and $\alpha_1 = 0.3225$, $\tau_1 = 0.9623$, $E_3 = 1.9637$, $a_{34} = 0.6509$, $b_{34} = 0.0278$, $E_4 = 2.1947$, $a_{43} = 1.4209$, $b_{43} = -0.0010$ and the initial condition $x_3(0) = 0.6258$, $v_3(0) = 0.3154$, $x_4(0) = 0.4318$, $v_4(0) = 0.0218$

most effective parameters are τ and α where the parameter τ stands for the number of oscillations. In order to verify the results, we repeated the optimization of human locomotion shown in Fig. 5 and 6 and started changing the value of τ: the results reveal two distinct patterns: the first unfolds an inverse pattern, where an increase in the value of τ results in a decrease in displacement and velocity. The second one, by contrast, reveals that a decrease in the value of τ produces an increase in

Table 1: Effects of τ on J_1 and x_b when other parameters are fixed

τ	J_1	x_b
0.9624	29.7447	1.0671
1.9624	430.0472	0.4366
2.9624	403.9559	0.2183
3.9624	466.4726	0.2156
0.5624	415.6542	1.6304
0.1624	359.8602	3.4021

Table 2: Effects of α on J_1 and x_b when other parameters are fixed

α	J_1	x_b
0.0020	34.0806	1.0502
0.0080	37.8369	1.0015
0.0180	49.4105	0.7352
0.0900	125.3871	0.1278

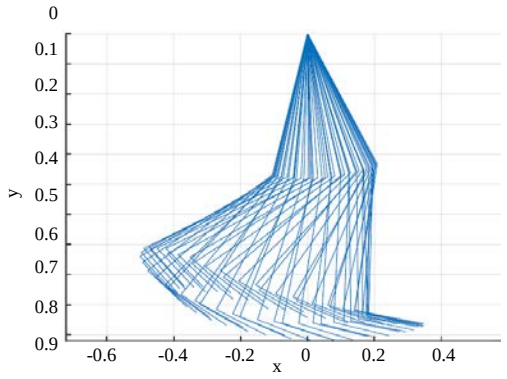

Fig. 17: One leg with 3 DOFs animation in the swing phase corresponding to the same values in Fig. 16

displacement and velocity. Table 1 summarizes these results where the values of the fixed parameters are $\alpha = 0.0010$, $E_1 = 0.4721$, $a_{12} = 1.6071$, $b_{12} = 0.0288$, $E_2 = 1.3746$, $a_{21} = 2.1200$, $b_{21} = -0.0479$.

In a similar fashion, an increase in the value of parameter α contributes to a decrease in the displacement and velocity. However, decreasing the value of α by a small amount results in an equal percentage increase in the displacement and velocity. These results are not inconsistent with the conclusions obtained from the stability section. Table 2 summarizes the results of increasing and decreasing the value of parameter α where the values of the fixed parameters are $\tau = 0.9624$, $E_1 = 0.4721$, $a_{12} = 1.6071$, $b_{12} = 0.0288$, $E_2 = 1.3746$, $a_{21} = 2.1200$, $b_{21} = -0.0479$.

In view of the fact that we used the GA for optimization, the outputs of the CPGs were not identical to the real results obtained for the hip and knee, however, they were almost identical. This small difference may be attributable to the facts that the Genetic algorithm only yielded the local minimum, the waist of the lower body in our model is parallel to the ground and the hip joint is fixed. To show the effect of the coupling weights a_{ij} and b_{ij}, we repeat the same experiment that is done in Table 1 and 2 by running the optimization and using the cost function J_1, the results are shown by Table 3-6. Table 3 presents the results of changing the couple weights a_{12}, b_{12} and τ. In this table, the values of the fixed parameters are $\alpha = 0.0010$, $E_1 = 0.4721$, $E_2 = 1.3746$, $a_{21} = 2.1200$, $b_{21} = -0.0479$. Note that, the errors between the real data and the outputs of the CPGs in Table 3 have decreased relative to Table 1.

Table 3: Values of J_1 and x_b for different choices of a_{12} and b_{12}

τ	a_{12}	b_{12}	J_1	x_b
0.9624	1.5071	0.0288	29.7447	1.0671
1.9624	1.5993	-0.1322	402.7306	-0.1514
2.9624	1.5889	-0.1820	382.4701	-0.1229
3.9624	1.5845	-0.2920	441.6822	-0.1467
0.5624	1.4999	0.0434	33.19570	1.0906
0.1624	1.5916	0.0086	318.3521	0.3164

Table 4: Values of J_1 and x_b for different choices of a_{21}, b_{21} and τ

τ	a_{21}	b_{21}	J_1	x_b
0.9624	2.1200	-0.0479	29.74470	1.0671
1.9624	2.0087	-0.2107	412.9008	-0.1514
2.9624	1.9999	-0.3484	385.4969	0.1865
3.9624	2.0474	-0.4382	448.4796	0.1493
0.5624	2.0650	-0.1311	388.3686	0.9846
0.1624	2.1228	-0.1216	337.6760	0.8460

Table 5: Values of J_1 and x_b for different choices of a_{12}, b_{12}, a_{21}, b_{21} and τ

τ	a_{12}	b_{12}	a_{21}	b_{21}	J_1	x_b
0.9624	1.5071	0.0288	2.1200	-0.0479	29.7447	1.0671
1.9624	1.4579	-3.2676	2.1651	2.6068	68.6185	0.4021
2.9624	1.5900	-1.7699	2.1651	2.6068	309.9797	0.0200
3.9624	1.5731	-3.1830	2.2245	3.8558	282.0600	0.0338
0.5624	1.6839	0.0275	2.0681	-0.2714	334.0745	-0.7710
0.1624	1.6210	0.0028	2.0515	-0.0736	310.0280	-0.6511

Table 6: Values of J_1 and x_b for different choices of a_{12}, b_{12}, a_{21}, b_{21} and α

α	a_{12}	b_{12}	a_{21}	b_{21}	J_1	x_b
0.0020	1.4950	0.0474	2.1256	-0.0398	32.8514	1.1122
0.0080	1.4729	0.0667	2.1262	-0.0291	33.2497	1.0495
0.0180	1.4535	0.1074	2.1254	-0.0019	38.2692	0.5752
0.0900	1.4719	0.4715	2.1231	0.2778	60.2143	0.0001
0.0005	1.5019	0.0428	2.1251	-0.0419	33.2938	1.1200
0.0001	1.5038	0.0415	2.1250	-0.0425	33.4570	1.1157

These results are similar to the coupling weights a_{21} and b_{21} as seen in Table 4. In this table the values of the fixed parameters are $\alpha = 0.0010$, $E_1 = 0.4721$, $E_2 = 1.3746$, $a_{12} = 1.5071$, $b_{12} = 0.0288$.

By changing the value of τ and the four parameters a_{12}, b_{12}, a_{21} and b_{21} as in Table 5 and following the same previous steps. In this table the values of the fixed parameters are $\alpha = 0.0010$, $E_1 = 0.4721$, $E_2 = 1.3746$. Note that the results presented in Table 5 are much better than those in Table 3 and 4.

By using the same technique and changing the value of α. The optimization is done for the bidirectional two CPGs in order to find the optimal values of parameters a_{12}, b_{12}, a_{21}, b_{21}. These results are illustrated in Table 6. In this table the values of the fixed parameters are $\tau = 0.9624$, $E_1 = 0.4721$, $E_2 = 1.3746$.

CONCLUSION

This study has recommended to the necessity for the study of human locomotion to explore in detail the underlying constraints that render the optimization of CPGs more practical, and it has presented the case for the adoption of a particular type of CPG, namely the bidirectional two CPGs which generates rhythmic patterns that are close most of those existing in real life. In light of the theoretical framework discussed above, the bidirectional two CPGs seem to be the best candidate to create rhythmic patterns most analogous to those derived from real data by using the Genetic Algorithm (GA) and pattern search solvers. Most importantly, the study shows that a small change in the parameter settings of CPGs may very well produce different results. The study also shows that an increase in the values of τ and α decreases the displacement and the velocity whereas a decrease in their values increases the displacement and the velocity. In conclusion, the parameters of the coupling weights are important in order to balance the disturbance during optimization. Moreover, when the parameters α and $\tau \in (0, 3)$, the bidirectional two CPGs of the third type are definitely able to generate different RPs for one leg to move; these RPs generate different types of locomotion when the couple parameters a_{ij} and $b_{ij} \in [-3, 3]$.

It is certain that it is possible to generate the rhythmic patterns by optimizing the bidirectional two CPGs outside of the above regions. This study indicates that not only do CPGs in the spinal cord of humans influence human locomotion, they also take over the locomotion without any provided sensory feedback. To the extent that bidirectional CPGs are the most effective essentials akin to real life-induced rhythmic patterns, it is reasonable for them to be considered pivotal features most conducive to locomotion.

REFERENCES

01. Ijspeert, A.J., 2008. Central pattern generators for locomotion control in animals and robots: A review. Neural Networks, 21: 642-653.
02. Yu, J., M. Tan, J. Chen and J. Zhang, 2013. A survey on CPG-inspired control models and system implementation. IEEE. Trans. Neural Networks Learn. Syst., 25: 441-456.
03. Billard, A. and A.J. Ijspeert, 2000. Biologically inspired neural controllers for motor control in a quadruped robot. Proceedings of the IEEE-INNS-ENNS International Joint Conference on Neural Networks Vol. 6, July, 27, 2000, IEEE, Los Angeles, California, ISBN:0-7695-0619-4, pp: 637-641.
04. Casasnovas, B. and P. Meyrand, 1995. Functional differentiation of adult neural circuits from a single embryonic network. J. Neurosci., 15: 5703-5718.
05. Vreeswijk, C., L.F. Abbott and E.G. Bard, 1994. When inhibition not excitation synchronizes neural firing. J. Comput. Neurosci., 1: 313-321.
06. Arikan, K.B. and B. Irfanoglu, 2011. A test bench to study bioinspired control for robot walking. J. Control Eng. Appl. Inf., 13: 76-80.
07. Elbori, A.E.G., M. Turan and K.B. Arıkan, 2017. Optimization of central patterns generators. J. Eng. Applied Sci., 12: 1164-1172.
08. Jiaqi, Z.H.A.N.G., T. Masayoshi, C.H.E.N. Qijun and L.I.U. Chengju, 2011. Dynamic walking of AIBO with Hopf oscillators. Chin. J. Mech. Eng., 24: 612-617.
09. Marbach, D., 2004. Evolution and online optimization of central pattern generators for modular robot locomotion. Master Thesis, Ecole Polytechnique Federale de Lausanne, Lausanne, Switzerland.
10. Williamson, M.M., 1999. Robot arm control exploiting natural dynamics. Ph.D. Thesis, Massachusetts Institute of Technology, Cambridge, Massachusetts.
11. Arena, P., L. Fortuna, M. Frasca and G. Sicurella, 2004. An adaptive, self-organizing dynamical system for hierarchical control of bio-inspired locomotion. IEEE. Trans. Syst. Man Cybern. B. (Cybern.), 34: 1823-1837.
12. Inagaki, S., H. Yuasa and T. Arai, 2003. CPG model for autonomous decentralized multi-legged robot system-generation and transition of oscillation patterns and dynamics of oscillators. Rob. Auton. Syst., 44: 171-179.
13. Ijspeert, A.J. and A. Crespi, 2007. Online trajectory generation in an amphibious snake robot using a lamprey-like central pattern generator model. Proceedings of the 2007 IEEE International Conference on Robotics and Automation, April 10-14, 2007, IEEE, Lausanne, Switzerland, ISBN:1-4244-0601-3, pp: 262-268.
14. Crespi, A. and A.J. Ijspeert, 2008. Online optimization of swimming and crawling in an amphibious snake robot. IEEE. Trans. Rob., 24: 75-87.
15. Taga, G., Y. Yamaguchi and H. Shimizu, 1991. Self-organized control of bipedal locomotion by neural oscillators in unpredictable environment. Biol. Cybern., 65: 147-159.
16. Taga, G., 1998. A model of the neuro-musculo-skeletal system for anticipatory adjustment of human locomotion during obstacle avoidance. Biol. Cybern., 78: 9-17.
17. Aoi, S. and K. Tsuchiya, 2005. Locomotion control of a biped robot using nonlinear oscillators. Auton. Robots, 19: 219-232.

18. Endo, G., J. Nakanishi, J. Morimoto and G. Cheng, 2005. Experimental studies of a neural oscillator for biped locomotion with QRIO. Proceedings of the 2005 IEEE International Conference on Robotics and Automation, April 18-22, 2005, IEEE, Kyoto, Japan, ISBN:0-7803-8914-X, pp: 596-602.
19. Torres-Huitzil, C. and B. Girau, 2008. Implementation of central pattern generator in an FPGA-based embedded system. Proceedings of the International Conference on Artificial Neural Networks, September 3-6, 2008, Springer, Prague, Czech Republic, pp: 179-187.
20. Bhatti, O.S., M. Rizwan, P.S. Shiokolas and B. Ali, 2019. Genetically optimized ANFIS-based PID controller design for posture-stabilization of self-balancing-robots under depleting battery conditions. J. Control Eng. Applied Inf., 21: 22-33.
21. Elbori, A.E.G., M. Turan and K.B. Arikan, 2018. Evaluation and optimization of nonlinear central pattern generators for robotic locomotion. J. Control Eng. Applied Inf., 20: 89-98.
22. Golden, J.A., 1990. Gait synthesis for the as-2 biped robot to climb stairs. Int. J. Robotics Automat., 5: 149-159.
23. Kajita, S. and K. Tani, 1991. Study of dynamic biped locomotion on rugged terrain-theory and basic experiment. Proceedings of the 5th International Conference on Advanced Robotics Robots in Unstructured Environments, June 19-22, 1991, IEEE, Pisa, Italy, pp: 741-746.
24. Kieboom, J.V.D., 2009. Biped locomotion and stability a practical approach. Master's Thesis, University of Groningen, Groningen, Netherlands.
25. Amrollah, E. and P. Henaff, 2010. On the role of sensory feedbacks in Rowat-Selverston CPG to improve robot legged locomotion. Front. Neurorob., 4: 113-113.